Supporting Information

"Optimization of a Pretargeted Strategy for the PET Imaging of Colorectal Carcinoma via the Modulation of Radioligand Pharmacokinetics"

Brian M. Zeglis[1], Christian Brand[2], Dalya Abdel-Atti[2], Kathryn E. Carnazza[2], Brendon E. Cook[1], Sean Carlin[2], Thomas Reiner[2], and Jason S. Lewis[2,3]

[1]Department of Chemistry and Biochemistry, Hunter College and the Graduate Center of the City University of New York, New York, NY, USA
[2]Department of Radiology, Memorial Sloan Kettering Cancer Center, New York, NY, USA
[3]Program in Molecular Pharmacology and Chemistry, Memorial Sloan Kettering Cancer Center, New York, NY, USA

Supplemental Methods

Instrumentation: All instruments were calibrated and maintained in accordance with standard quality-control procedures. UV-Vis measurements were taken on a Thermo Scientific NanoDrop 2000 Spectrophotometer. NMR spectroscopy was performed on a Bruker 500 MHz NMR with TopSpin 2.1 software for spectrum analysis. Electrospray ionization mass spectrometry (ESI-MS) spectra were recorded with a Waters Acquity UPLC (Milford, CA) with electrospray ionization SQ detector. High-resolution mass spectrometry (HRMS) spectra were recorded with a Waters LCT Premier system (ESI). Activity measurements were made using a Capintec CRC-15R Dose Calibrator (Capintec, Ramsey, NJ). For accurate quantification of activities, experimental samples were counted for 1 min on a calibrated Perkin Elmer (Waltham, MA) Automatic Wizard Gamma Counter. Labeling of antibodies with ^{64}Cu-labeled tetrazine radioligands was monitored using silica-gel impregnated glass-fiber instant thin-layer chromatography paper (Pall Corp., East Hills, NY) and analyzed on a Bioscan AR-2000 radio-TLC plate reader using Winscan Radio-TLC software (Bioscan Inc., Washington, D. C.).

HPLC: All HPLC purifications (6.0 mL/min, Buffer A: 0.1% TFA in water, Buffer B: 0.1% TFA in CH_3CN) were performed on a Shimadzu UFLC HPLC system equipped with a DGU-20A degasser, a SPD-M20A UV detector, a LC-6AB pump system, a CBM-20A communication BUS module, and a FRC-10A fraction collector using a C_{18} reversed phase XTerra® Preparative MS OBD™ column (10 μm, 19.2 mm × 250 mm) or a C_{18} reversed phase semi-Prep Phenomenex® Jupiter column (5 μm, 10 mm × 250 mm). Quality controls of synthesized compounds were performed using a C_{18} reversed phase Atlantis® T3 column (5 μm, 4.6 mm × 250 mm). All radio-HPLC analysis and purification experiments were performed using a Shimadzu HPLC equipped with a C_{18} reversed phase column (Phenomenex Luna analytical 4.6 x 250 mm), 2 LC-10AT pumps, a SPD-M10AVP photodiode array detector, a Bioscan Flow Counts radioactivity detector, and a gradient of 5:95 CH_3CN:H_2O (both with 0.1% TFA) to 95:5 CH_3CN:H_2O over 15 min.

Synthesis of Tz-PEG$_7$-AF680: Tz-PEG$_7$-NH_2 (1 mg; 0.0015 mmol; 651.8 g/mol) was dissolved in 400 μL DMSO and added to 2 mg AF680-NHS (.0017 mmol; 1.1 equiv.; ~1150 g/mol). 10 μL triethylamine (7.3 mg; 0.072 mmol; 101.2 g/mol) was then added to this solution, and the solution was placed on an agitating thermomixer at 300 rpm for 30 minutes at room temperature. After 30 minutes, the reaction was purified via preparative C_{18} HPLC using a gradient of 5:95 CH_3CN:H_2O (both with 0.1% TFA) to 95:5 CH_3CN:H_2O over 30 min (t_R = 11.2 min). Lyophilization of the HPLC eluent yielded the purified product as a 2 mg of a bright orange powder (MW ~1750; ~0.0011 mmol; ~75% yield).

Preparation of huA33-TCO: huA33 (2 mg, 13.3 nmol) was dissolved in 500 μL of phosphate buffered saline (PBS, pH 7.4), and the pH of the solution was adjusted to 8.8-9.0 with $NaHCO_3$ (0.1 M). To this solution was added an appropriate volume of TCO-NHS in DMF (10 mg/mL) to yield a TCO-NHS:huA33 reaction stoichiometry of 10:1. The resulting solution was incubated with gentle shaking for 30 min at room temperature. After 30 min, the modified antibody was purified using size-exclusion chromatography (Sephadex G-25 M, PD-10 column, GE Healthcare; dead volume = 2.5 mL, eluted with 500 mL fractions of PBS, pH 7.4) and concentrated with centrifugal filtration units with a 50,000 molecular weight cut off (Amicon™ Ultra 4, Millipore Corp., Billerica, MA) and PBS (pH 7.4).

Determination of the TCO occupancy of huA33-TCO: A solution of huA33-TCO (100 μg; 0.66 nmol) in 900 μL PBS (pH 7.4) was first prepared (0.74 μM). To this solution, 100 μL of a 1 mM solution of Tz-PEG$_7$-AF680 in DMSO was added to create a reaction solution of 1000 μL and concentrations of 0.66 μM

huA33-TCO and 100 μM Tz-PEG_7-AF680 (a ~150 fold excess of Tz). This solution was placed on an agitating thermomixer at 300 rpm for 180 minutes at room temperature. After incubation, the resulting fluorophore-labeled immunoconjugate was purified using size-exclusion chromatography (Sephadex G-25 M, PD-10 column, GE Healthcare; dead volume = 2.5 mL, eluted with 500 mL fractions of PBS, pH 7.4) and concentrated with centrifugal filtration units with a 50,000 molecular weight cut off (Amicon™ Ultra 4, Millipore Corp., Billerica, MA) and PBS (pH 7.4). The degree of labeling (DOL) was determined via UV-Vis. Absorbance measurements were taken at 280 nm and 680 nm for three separate antibody concentrations. The DOL was calculated using the following formulas:

$$A_{mAb} = A_{280} - A_{max}(CF)$$

$$DOL = [A_{max} * MW_{mAb}]/[[mAb] * \varepsilon_{AF680}]$$

where the correction factor (CF) for AF680 was given as 0.05 by the supplier, MW_{huA33} = 150,000, ε_{AF680} = 184,000, and $\varepsilon_{280,\,mAb}$ = 225,000. Given the rapid and quantitative nature of the IEDDA reaction, the degree of labeling of AF680 was assumed to be the degree of labeling of TCO.

Determination of Partition Coefficient: ^{64}Cu-Tz-PEG_7-NOTA, ^{64}Cu-Tz-NOTA, or ^{64}Cu-Tz-SarAr (1 μCi) was added to a mixture of 3 mL PBS (pH 7.4) and 3 mL 1-octanol. The resulting mixture was then vortexed thoroughly for 10 minutes and subsequently centrifuged at 1,000 rpm for 10 min. 1 mL of each layer (PBS and 1-octanol) was then collected, and the amount of radioactivity in each sample was counted on a gamma counter calibrated for ^{64}Cu. The partition coefficient (logD) was calculated using the formula:

$$\text{Log D} = \log_{10}[(\text{counts}_{\text{octanol}})/(\text{counts}_{\text{PBS}}]$$

All experiments were performed in triplicate.

Reaction of ^{64}Cu-Tz radioligands with huA33-TCO: In order to check their reactivity with TCO, ^{64}Cu-Tz-PEG_7-NOTA and ^{64}Cu-Tz-SarAr were added to a solution of huA33 in PBS (500 μL, pH 7.4) at a molar ratio of Tz:mAb of 1:1. The resulting solution was placed on an agitating thermomixer at 300 rpm for 30 minutes at room temperature. After this incubation, the progress of the reaction was assayed using radio-TLC with reverse-phase C_{18} TLC plates and a mobile phase of 1:1 CH_3CN:water (each with 0.1% TFA). Under these conditions, the ^{64}Cu-labeled antibody will remain at the baseline, while the ^{64}Cu-Tz-labeled radioligands will travel up the plate. If the purified radioimmunoconjugate is desired, the ^{64}Cu-Tz-huA33 was then purified using size-exclusion chromatography (Sephadex G-25 M, PD-10 column, GE Healthcare; dead volume = 2.5 mL, eluted with 500 mL fractions of PBS, pH 7.4). Typically, crude radiochemical yields of 90-95% were obtained, and post-purification radiochemical purities were >99% (corresponding to specific activities of 2.0-2.5 mCi/mg; 74-92.5 MBq/mg). All experiments were performed in triplicate.

PBS and Serum Stability of ^{64}Cu-Tz-PEG_7-NOTA and ^{64}Cu-Tz-SarAr: ^{64}Cu-Tz-PEG_7-NOTA and ^{64}Cu-Tz-SarAr (1000 μCi) were incubated on an agitating thermomixer (300 rpm) at 37 °C in 500 μL of either PBS (pH 7.4) or human serum. At each prescribed time-point, 100 μL of the solution was removed and placed into a 1.7 mL microcentrifuge tube. For the PBS samples, the compound was injected directly onto the HPLC and analyzed using a gradient of 5:95 CH_3CN:H_2O (both with 0.1% TFA) to 95:5 CH_3CN:H_2O over 15 min. For the serum samples, 100 μL cold CH_3CN was added to the serum, and the resultant mixture was vortexed and centrifuged at 10,000 rpm for 10 min. After this, the clear supernatant was removed, moved to a new 1.7 mL microcentrifuge tube, and centrifuged again at 10,000 rpm for 10 min. The clear supernatant from this second spin was then injected into the HPLC and analyzed using a gradient of 5:95 CH_3CN:H_2O (both with 0.1% TFA) to 95:5 CH_3CN:H_2O over 15 min. The residual protein from the centrifuge spins was checked for radioactivity, and only minimal residual activity remained (<1% of the starting ^{64}Cu for each ^{64}Cu-Tz-PEG_7-NOTA and ^{64}Cu-Tz-SarAr). The fraction of intact ^{64}Cu-Tz-PEG_7-NOTA or ^{64}Cu-Tz-SarAr was determined by integrating the peak corresponding to the compound (t_R = 9.7 and 8.7 minutes, respectively) and dividing by the integral over the whole HPLC run. Both the injection loop and column were monitored to detect the presence of residual activity. All experiments were performed in triplicate.

In Vivo Stability of ^{64}Cu-Tz-SarAr: Healthy athymic nude mice were injected with ^{64}Cu-Tz-SarAr (300-350 μCi) via intravenous tail vein injection. After 15 min, 1 h, or 4 h, the mice were sacrificed via CO_2 asphyxiation, and their blood (500 μL) was collected via cardiac puncture in heparinized 1.7 mL

microcentrifuge tubes. These tubes were then centrifuged at 10,000 rpm for 10 minutes to separate plasma from red-blood cells. After 10 minutes, the plasma supernatant was then transferred to a new 1.7 mL microcentrifuge tube and placed on ice. Subsequently, 500 μL of ice-cold CH_3CN was added to the plasma to precipitate the proteins, and the tubes were vortexed briefly and centrifuged again for 10 min at 10,000 rpm. After this centrifugation, the supernatant was carefully removed and transferred to another 1.7 mL microcentrifuge tube, in which it was subjected to another round of centrifugation at 10,000 rpm for 10 min. After this final centrifugation, the supernatant was again transferred to a clean 1.7 mL microcentrifuge tube. This solution was then analyzed via radio-TLC methods using reverse-phase C_{18} TLC plates and a mobile phase of 1:1 CH_3CN:water (each with 0.1% TFA). Using this method, any free $^{64}Cu^{2+}$ will remain at the baseline, while ^{64}Cu-Tz-SarAr and other metabolites will travel up the TLC plate. The fraction of intact ^{64}Cu-Tz-SarAr was calculated by dividing the integral of the parent compound peak over the integral of the entire radio-TLC chromatogram. All experiments were performed in triplicate.

Cell Culture: Human colorectal cell line SW1222 was obtained from the Ludwig Institute of Cancer Research and maintained in Iscove's Modified Dulbecco's Medium, supplemented with 10% heat-inactivated fetal calf serum, 2.0 mM glutamine, 100 units/mL penicillin, and 100 units/mL streptomycin in a 37°C environment containing 5% CO_2. Cell lines were harvested and passaged weekly using a formulation 0.25% trypsin/0.53 mM EDTA in Hank's Buffered Salt Solution without calcium and magnesium.

Xenograft Models: All animal experiments were performed under an Institutional Animal Care and Use Committee-approved protocol, and the experiments followed institutional guidelines for the proper and humane use of animals in research. Six to eight week-old athymic nude female mice were obtained from Charles River Laboratories (Wilmington, MA). Animals were housed in ventilated cages, were given food and water *ad libitum*, and were allowed to acclimatize for approximately 1 week prior to inoculation. SW1222 tumors were induced on the right shoulder by a subcutaneous injection of 5.0 x 10^6 cells in a 150 μL cell suspension of a 1:1 mixture of fresh media:BD Matrigel (BD Biosciences, Bedford, Ma). The xenografts reached ideal size for imaging and biodistribution (~100-150 mm^3) in approximately 18-21 days.

Immunoreactivity Assays: Immunoreactivity assays employing the huA33-TCO antibodies labeled with the ^{64}Cu-Tz radioligands were performed as previously reported using A33 antigen-expressing SW1222 human colorectal cancer cells.[1-2] All experiments were performed in triplicate.

PET Imaging with ^{64}Cu-Labeled Tetrazine Radioligands: All PET imaging experiments were performed on an Inveon PET/CT scanner (Siemens Healthcare Global). Healthy female athymic nude mice (n = 4 per radioligand) were administered ^{64}Cu-Tz-NOTA, ^{64}Cu-Tz-PEG_7-NOTA, or ^{64}Cu-Tz-SarAr (300-350 μCi in 200 μL 0.9% sterile saline) via intravenous tail vein injection (t = 0). Approximately 5 minutes prior to the PET images, mice were anesthetized by inhalation of 2% isoflurane (Baxter Healthcare, Deerfield, IL)/oxygen gas mixture and placed on the scanner bed; anesthesia was maintained using 1% isoflurane/gas mixture. Static scans were recorded at various time points after injection with a minimum of 30 million coincident events (10-30 min total scan time). An energy window of 350-700 keV and a coincidence timing window of 6 ns were used. Data were sorted into 2-dimensional histograms by Fourier re-binning, and the images were reconstructed using a two-dimensional ordered subset expectation maximization (2DOSEM) algorithm (16 subsets, 4 iterations) into a 128 × 128 × 159 (0.78 × 0.78 × 0.80 mm) matrix. The image data was normalized to correct for non-uniformity of response of the PET, dead-time count losses, positron branching ratio, and physical decay to the time of injection but no attenuation, scatter, or partial-volume averaging correction was applied. Activity concentrations (percentage of dose per gram of tissue [%ID/g]) and maximum intensity projections were determined by conversion of the counting rates from the reconstructed images. All of the resulting PET images were analyzed using ASIPro VM™ software.

Acute Biodistribution with ^{64}Cu-Labeled Tetrazine Radioligands: Healthy female athymic nude mice were administered ^{64}Cu-Tz-PEG_7-NOTA or ^{64}Cu-Tz-SarAr (25-30 μCi in 200 μL 0.9% sterile saline) via intravenous tail vein injection (t = 0). Animals (n = 4 per group) were euthanized by CO_2(g) asphyxiation at 1, 4, 12, and 24 h after injection. After asphyxiation, tissues were removed, rinsed in water, dried in air for 5 min, weighed, and counted in a gamma counter calibrated for ^{64}Cu. Counts were converted into activity using a calibration curve generated from known standards. Count data were background- and decay-corrected to the time of injection, and the percent injected dose per gram (%ID/g) for each tissue sample was calculated by normalization to the total activity injected.

Ex Vivo Autoradiography, Immunohistochemistry, and Histology: Following PET imaging, tumors were excised and embedded in optimal-cutting-temperature mounting medium (OCT, Sakura Finetek) and frozen on dry ice. Series of 10 μm frozen sections were then cut. To determine radiotracer distribution, digital autoradiography was performed by placing tissue sections in a film cassette against a phosphor imaging plate (Fujifilm BAS-MS2325; Fuji Photo Film) for an appropriate exposure period at −20°C. Phosphor imaging plates were read at a pixel resolution of 25 μm with a Typhoon 7000 IP plate reader (GE Healthcare). After autoradiographic exposure, the same frozen sections were then used for fluorescence staining and microscopy. Immunofluorescence staining and imaging of A33 was performed essentially as previously described.[3] Frozen sections were fixed in 4% paraformaldehyde, and subsequently incubated with huA33 primary antibody (5μg/ml) overnight at 4°C, followed by secondary detection using goat anti-human Alexa-568 for 1 h at room temperature (20 μg/ml, Molecular Probes). Whole mount fluorescence images were acquired at ×40 magnification using a BX60 fluorescence microscope (Olympus America, Inc.) equipped with a motorized stage (Prior Scientific Instruments Ltd.) and CC12 camera (Olympus). Whole-tumor montage images were obtained by acquiring multiple fields at ×40 magnification, followed by alignment using MicroSuite Biologic Suite (version 2.7; Olympus). Fluorescence and autoradiographic images were registered using Adobe Photoshop (CS6) as previously described.[4]

Dosimetry: Mouse biodistribution data were expressed as normal-organ mean standard uptake values (SUVs) versus time post-administration. Assuming, in first order, that SUVs are independent of body mass and thus the same among species, the mean SUV in mouse organ i, $SUV_{Organ\ i|Mouse}$, was converted to the fraction of the injected dose in each human organ I, $FID_{Organ\ I|Human}$, using the following formula

$$FID_{Organ\ i|Human} = SUV_{ran\ i|Mouse} \bullet \frac{\text{Mass of Human Organ i}}{\text{Mass of Human Total Body}}$$

and the organ and total-body masses of the 70-kg Standard Man anatomic model.[5] These data (corrected for radioactive decay to the time of injection) were then fit to a mono-exponential or bi-exponential time-activity function, depending on the organ. The cumulated activity, or residence time, in human organ i, t_i, in μCi-h/μCi, was then calculated by analytically integrating the time-activity function in organ i, replacing the biological clearance constant, $(l_b)_j$. for each component j of the fitted exponential function with the corresponding effective clearance constant, $(l_e)_j = (l_b)_j + l_p$, where l_p is the physical decay constant of the radionuclide. The resulting organ residence times were entered into the OLINDA computer program to yield the mean organ absorbed doses and effective dose in rad/mCi and rem/mCi, respectively.[6]

Statistical Analysis: Data were analyzed by the unpaired, two-tailed Student's t-test. Differences at the 95% confidence level ($P < 0.05$) were considered to be statistically significant.

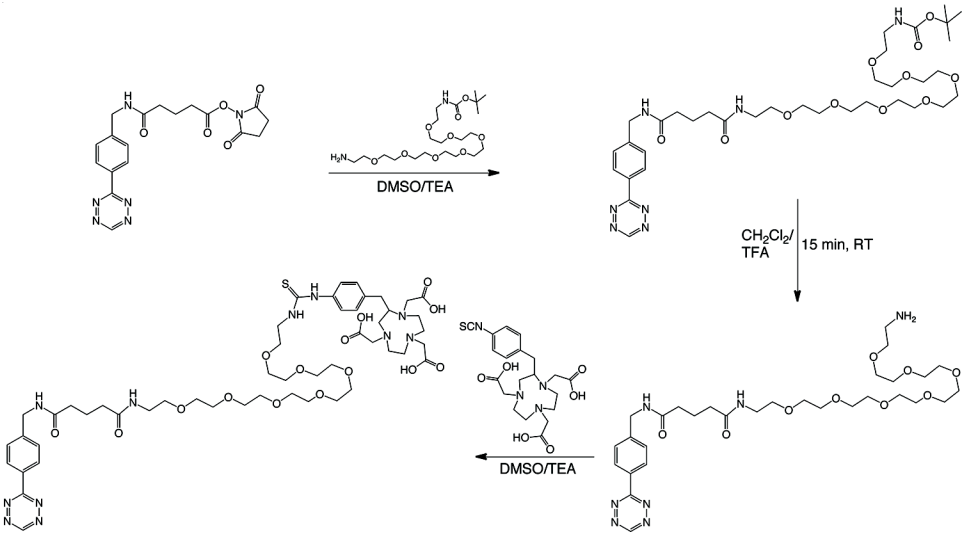

Figure S1. Schematic of the synthesis of Tz-PEG$_7$-NOTA

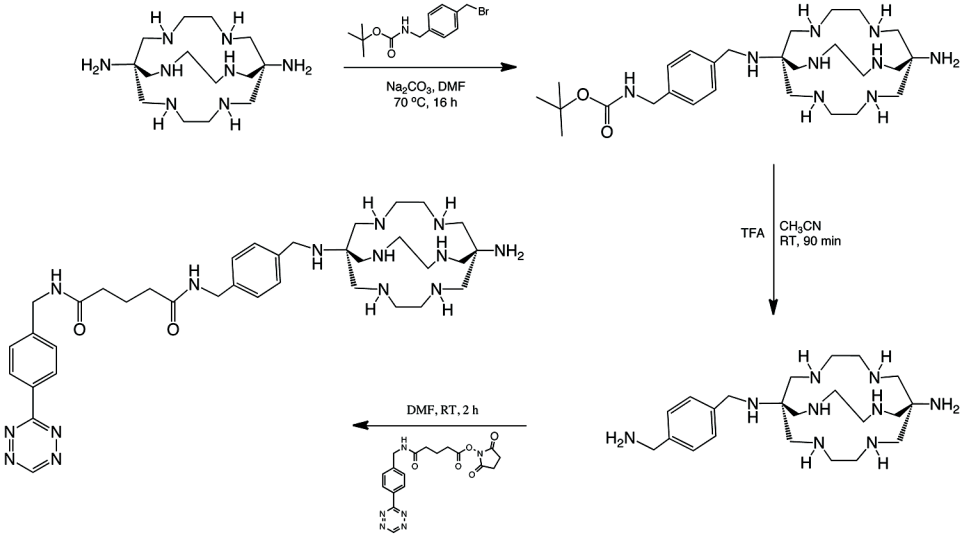

Figure S2. Schematic of the synthesis of Tz-SarAr

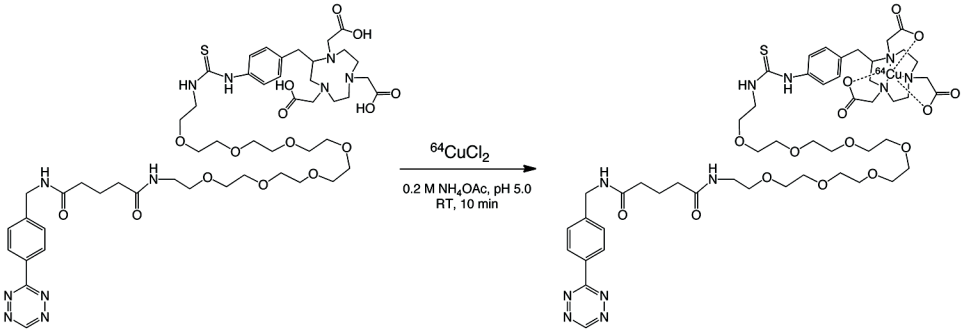

Figure S3. Schematic of the radiosynthesis of ^{64}Cu-Tz-PEG$_7$-NOTA

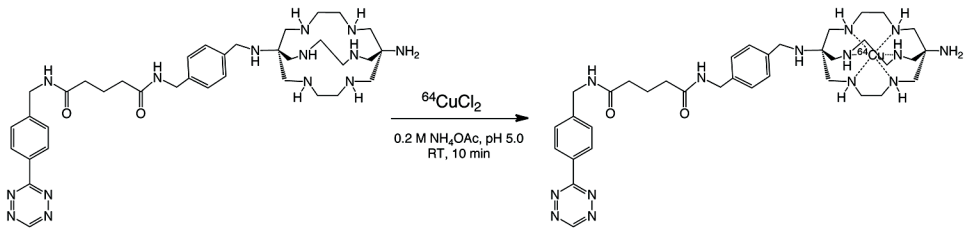

Figure S4. Schematic of the radiosynthesis of ^{64}Cu-Tz-SarAr

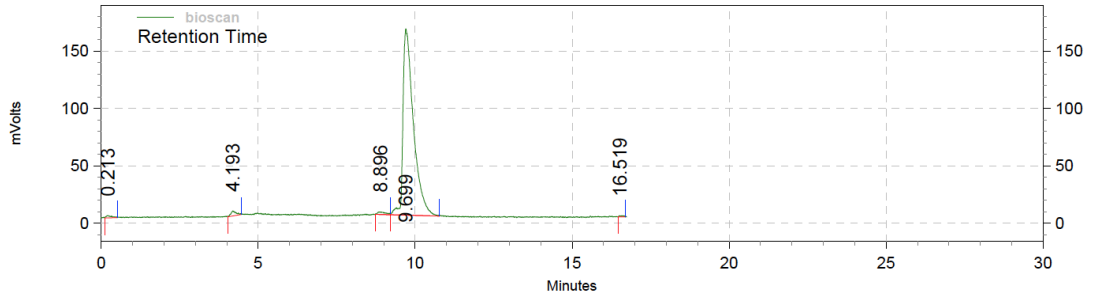

Figure S5. Crude radio-HPLC chromatogram of ^{64}Cu-Tz-PEG$_7$-NOTA

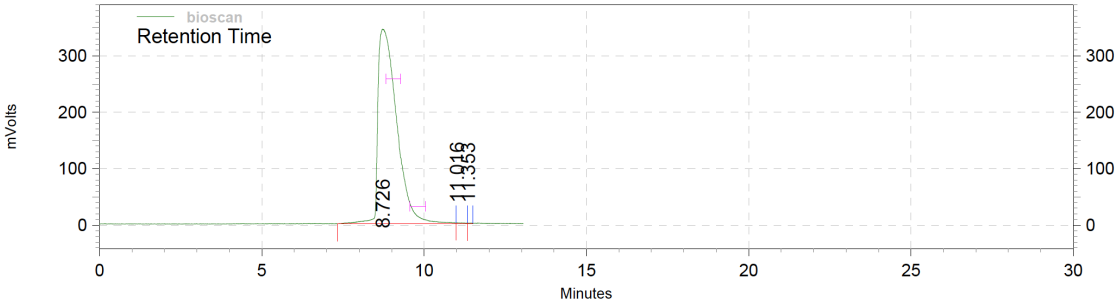

Figure S6. Crude radio-HPLC chromatogram of ^{64}Cu-Tz-SarAr

Radioligand	LogD
^{64}Cu-Tz-NOTA	-2.54 ± 0.10
^{64}Cu-Tz-PEG$_7$-NOTA	-2.44 ± 0.08
^{64}Cu-Tz-SarAr	-2.08 ± 0.06

Table S1. Partition coefficient (LogD) of the ^{64}Cu-labeled tetrazines in 1-octanol and PBS (pH 7.4)

Time	^{64}Cu-Tz-PEG$_7$-NOTA	^{64}Cu-Tz-SarAr
2 h	87.0 ± 1.3	94.7 ± 0.6
4 h	83.2 ± 4.6	93.3 ± 0.5
8 h	76.2 ± 2.6	89.7 ± 2.3

Table S2. Percent of ^{64}Cu-Tz-PEG$_7$-NOTA and ^{64}Cu-Tz-SarAr intact after incubation in PBS (pH 7.4) at 37 °C

Time	^{64}Cu-Tz-PEG$_7$-NOTA	^{64}Cu-Tz-SarAr
2 h	84.7 ± 4.8	92.0 ± 2.1
4 h	77.8 ± 3.5	81.2 ± 3.7
8 h	64.0 ± 6.5	67.7 ± 4.3

Table S3. Percent of ^{64}Cu-Tz-PEG$_7$-NOTA and ^{64}Cu-Tz-SarAr intact after incubation in human serum at 37 °C

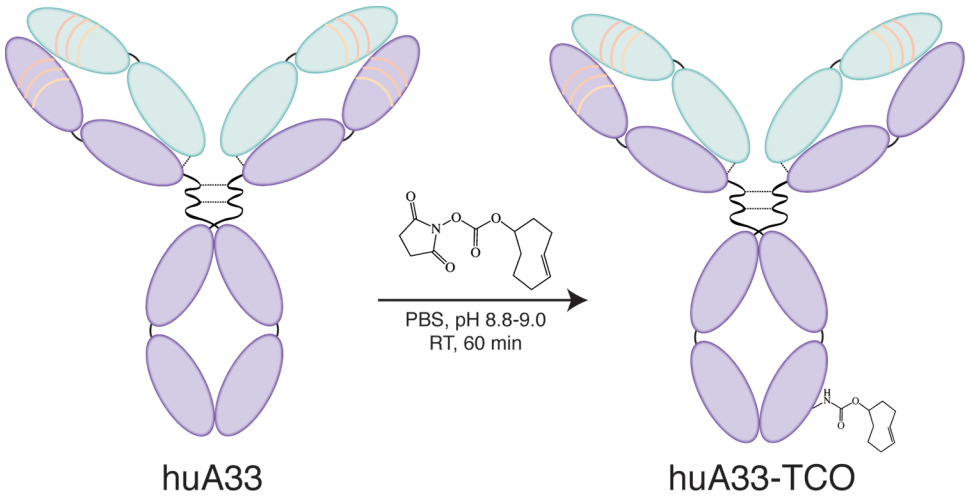

Figure S7. Schematic of the synthesis of huA33-TCO

Radioimmunoconjugate	Immunoreactive Fraction
huA33-TCO + ^{64}Cu-Tz-PEG$_7$-NOTA	0.96 ± 0.02
huA33-TCO + ^{64}Cu-Tz-SarAr	0.97 ± 0.01

Table S4. Immunoreactive fractions of radioimmunoconjugates formed through the reaction of huA33-TCO and either ^{64}Cu-Tz-PEG$_7$-NOTA or ^{64}Cu-Tz-SarAr, as determined via *in vitro* assays with A33 antigen-expressing SW1222 cells

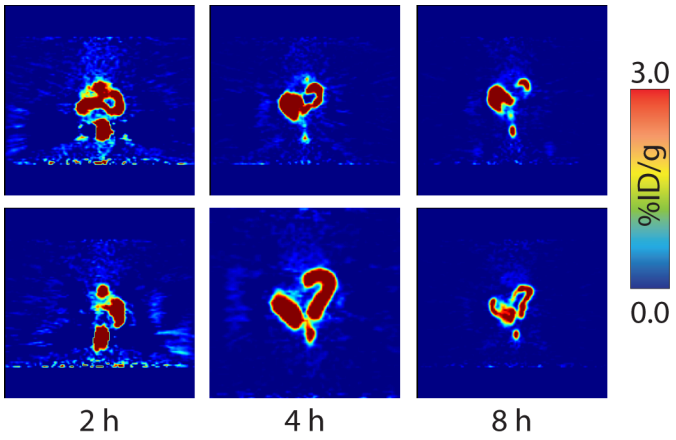

Figure S8. PET imaging data for ^{64}Cu-Tz-NOTA in two healthy mice. Healthy female athymic nude mice were administered ^{64}Cu-Tz-NOTA (300-350 μCi in 200 μL 0.9% sterile saline) via intravenous tail vein injection (t = 0). Approximately 5 minutes prior to the PET images, mice were anesthetized by inhalation of 2% isoflurane (Baxter Healthcare, Deerfield, IL)/oxygen gas mixture and placed on the scanner bed; anesthesia was maintained using 1% isoflurane/gas mixture. Static scans were recorded at various time points after injection with a minimum of 30 million coincident events (10-30 min total scan time). Activity concentrations (percentage of dose per gram of tissue [%ID/g]) and maximum intensity projections were determined by conversion of the counting rates from the reconstructed images. All of the resulting PET images were analyzed using ASIPro VM™ software. The coronal slices above are representative images chosen to illustrate the areas of highest uptake.

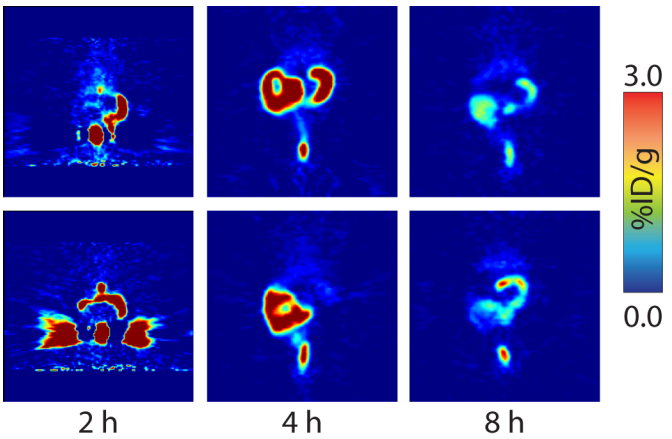

Figure S9. PET imaging data for ^{64}Cu-Tz-PEG$_7$-NOTA in two healthy mice. Healthy female athymic nude mice were administered ^{64}Cu-Tz-PEG$_7$-NOTA (300-350 μCi in 200 μL 0.9% sterile saline) via intravenous tail vein injection (t = 0). Approximately 5 minutes prior to the PET images, mice were anesthetized by inhalation of 2% isoflurane (Baxter Healthcare, Deerfield, IL)/oxygen gas mixture and placed on the scanner bed; anesthesia was maintained using 1% isoflurane/gas mixture. Static scans were recorded at various time points after injection with a minimum of 30 million coincident events (10-30 min total scan time). Activity concentrations (percentage of dose per gram of tissue [%ID/g]) and maximum intensity projections were determined by conversion of the counting rates from the reconstructed images. All of the resulting PET images were analyzed using ASIPro VM™ software. The coronal slices above are representative images chosen to illustrate the areas of highest uptake.

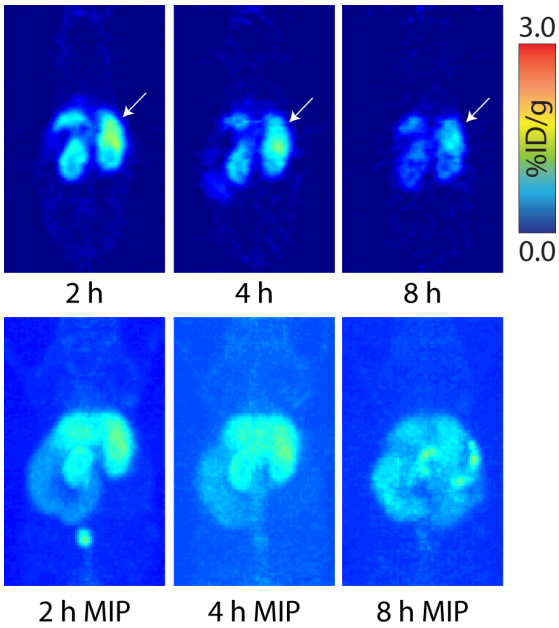

Figure S10. PET imaging data for ^{64}Cu-Tz-SarAr in a healthy mouse. Healthy female athymic nude mice were administered ^{64}Cu-Tz-SarAr (300-350 μCi in 200 μL 0.9% sterile saline) via intravenous tail vein injection (t = 0). Approximately 5 minutes prior to the PET images, mice were anesthetized by inhalation of 2% isoflurane (Baxter Healthcare, Deerfield, IL)/oxygen gas mixture and placed on the scanner bed; anesthesia was maintained using 1% isoflurane/gas mixture. Static scans were recorded at various time points after injection with a minimum of 30 million coincident events (10-30 min total scan time). Activity concentrations (percentage of dose per gram of tissue [%ID/g]) and maximum intensity projections were determined by conversion of the counting rates from the reconstructed images. All of the resulting PET images were analyzed using ASIPro VM™ software. Maximum intensity projections (MIPs) are shown for each time point, and the coronal slices above are representative images chosen to illustrate the areas of highest uptake (*i.e.* the kidneys, white arrow),

	1 h	**4 h**	**24 h**
Blood	0.23 ± 0.01	0.13 ± 0.01	0.07 ± 0.01
Heart	0.10 ± 0.02	0.11 ± 0.02	0.09 ± 0.01
Lung	0.38 ± 0.06	0.27 ± 0.08	0.21 ± 0.02
Liver	1.45 ± 0.39	0.42 ± 0.13	0.21 ± 0.06
Spleen	0.15 ± 0.05	0.09 ± 0.02	0.08 ± 0.02
Stomach	0.12 ± 0.04	0.05 ± 0.03	0.18 ± 0.11
Large Intestine	11.58 ± 2.19	10.03 ± 1.33	1.37 ± 0.65
Small Intestine	3.14 ± 1.47	0.17 ± 0.07	0.10 ± 0.02
Kidney	0.53 ± 0.09	0.33 ± 0.07	0.22 ± 0.07
Muscle	0.04 ± 0.02	0.03 ± 0.02	0.03 ± 0.03
Bone	0.10 ± 0.03	0.07 ± 0.04	0.03 ± 0.01

Table S5. Biodistribution data (%ID/g ± SD) of ^{64}Cu-Tz-NOTA versus time in healthy athymic nude (n = 4 for each time point). Mice were administered ^{64}Cu-Tz-NOTA (25-30 μCi in 200 μL 0.9% sterile saline) via intravenous tail vein injection. Animals were euthanized by CO_2(g) asphyxiation at 1, 4, and 24 h after injection. After asphyxiation, tissues were removed, rinsed in water, dried in air for 5 min, weighed, and counted in a gamma counter calibrated for ^{64}Cu. Counts were converted into activity using a calibration curve generated from known standards. Count data were background- and decay-corrected to the time of injection, and the percent injected dose per gram (%ID/g) for each tissue sample was calculated by normalization to the total activity injected. Stomach, small intestine, and large intestine measurements include contents.

	1 h	4 h	24 h
Blood	0.38 ± 0.14	0.26 ± 0.14	0.08 ± 0.01
Heart	0.17 ± 0.02	0.18 ± 0.03	0.09 ± 0.01
Lung	0.49 ± 0.11	0.35 ± 0.13	0.17 ± 0.03
Liver	0.77 ± 0.11	0.63 ± 0.2	0.32 ± 0.11
Spleen	0.19 ± 0.01	0.14 ± 0.02	0.12 ± 0.01
Stomach	0.18 ± 0.06	0.36 ± 0.25	0.09 ± 0.02
Large Intestine	6.35 ± 0.69	4.91 ± 0.71	0.40 ± 0.15
Small Intestine	0.5 ± 0.26	0.3 ± 0.14	0.10 ± 0.01
Kidney	1.51 ± 0.24	1.23 ± 0.39	0.86 ± 0.11
Muscle	0.05 ± 0.01	0.03 ± 0.02	0.02 ± 0.01
Bone	0.09 ± 0.06	0.07 ± 0.02	0.06 ± 0.01

Table S6. Biodistribution data (%ID/g ± SD) of ^{64}Cu-Tz-PEG$_7$-NOTA versus time in healthy athymic nude (n = 4 for each time point). Mice were administered ^{64}Cu-Tz-PEG$_7$-NOTA (25-30 μCi in 200 μL 0.9% sterile saline) via intravenous tail vein injection. Animals were euthanized by CO_2(g) asphyxiation at 1, 4, and 24 h after injection. After asphyxiation, tissues were removed, rinsed in water, dried in air for 5 min, weighed, and counted in a gamma counter calibrated for ^{64}Cu. Counts were converted into activity using a calibration curve generated from known standards. Count data were background- and decay-corrected to the time of injection, and the percent injected dose per gram (%ID/g) for each tissue sample was calculated by normalization to the total activity injected. Stomach, small intestine, and large intestine measurements include contents.

	1 h	4 h	24 h
Blood	0.42 ± 0.11	0.15 ± 0.01	0.06 ± 0.01
Heart	0.22 ± 0.06	0.12 ± 0.02	0.08 ± 0.02
Lung	0.32 ± 0.06	0.31 ± 0.09	0.24 ± 0.06
Liver	0.72 ± 0.03	0.42 ± 0.24	0.28 ± 0.07
Spleen	0.38 ± 0.06	0.2 ± 0.05	0.21 ± 0.04
Stomach	0.24 ± 0.14	0.2 ± 0.1	0.05 ± 0.01
Large Intestine	0.07 ± 0.01	0.08 ± 0.03	0.07 ± 0.01
Small Intestine	0.29 ± 0.21	0.16 ± 0.03	0.07 ± 0.01
Kidney	2.34 ± 0.35	1.57 ± 0.19	1.26 ± 0.41
Muscle	0.05 ± 0.03	0.04 ± 0.01	0.03 ± 0.01
Bone	0.12 ± 0.03	0.09 ± 0.01	0.08 ± 0.02

Table S7. Biodistribution data (%ID/g ± SD) of ^{64}Cu-Tz-SarAr versus time in healthy athymic nude (n = 4 for each time point). Mice were administered ^{64}Cu-Tz-SarAr (25-30 μCi in 200 μL 0.9% sterile saline) via intravenous tail vein injection. Animals were euthanized by CO_2(g) asphyxiation at 1, 4, and 24 h after injection. After asphyxiation, tissues were removed, rinsed in water, dried in air for 5 min, weighed, and counted in a gamma counter calibrated for ^{64}Cu. Counts were converted into activity using a calibration curve generated from known standards. Count data were background- and decay-corrected to the time of injection, and the percent injected dose per gram (%ID/g) for each tissue sample was calculated by normalization to the total activity injected. Stomach, small intestine, and large intestine measurements include contents.

Time	Activity in Blood (%ID/g)
15 min	3.02 ± 1.10
30 min	1.55 ± 0.21
1 h	0.42 ± 0.11
4 h	0.15 ± 0.01
12 h	0.12 ± 0.03
24 h	0.06 ± 0.01

Table S8. The *in vivo* blood residence time of ^{64}Cu-Tz-SarAr in healthy athymic nude mice (n = 3).

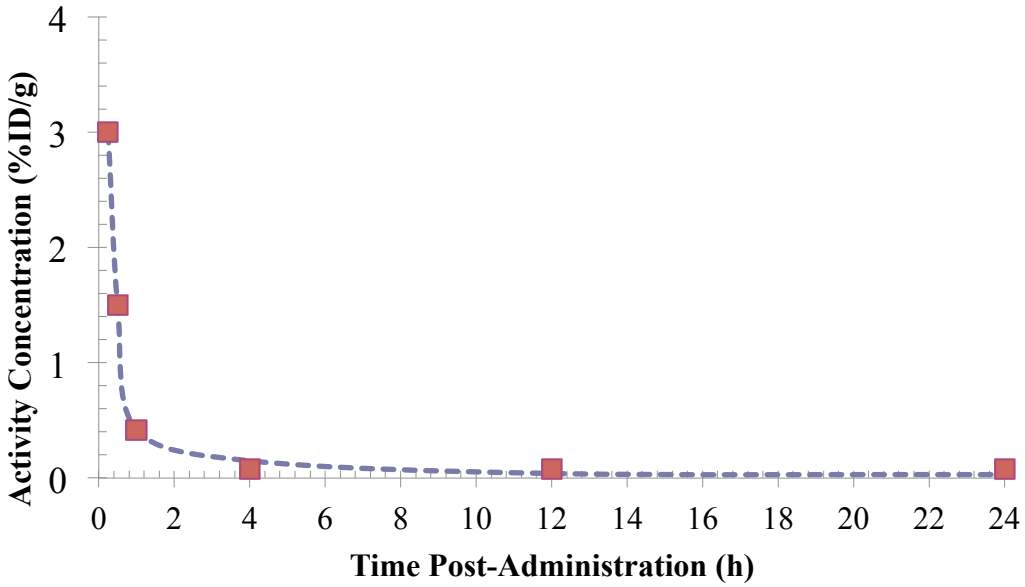

Figure S11. Plot of the clearance of ^{64}Cu-Tz-SarAr from the blood vs. time (red squares). Fitting of the data points to a biexponential function (dotted line) reveals that >99% of the radioligand clears from the blood with a half-life of ~16 minutes.

Time	% Intact ^{64}Cu-Tz-SarAr
15 min	96.8 ± 0.8
1 h	82.0 ± 3.3
4 h	29.0 ± 5.9

Table S9. Percent of ^{64}Cu-Tz-SarAr intact in blood after vs. time. These numbers are generally favorably comparable to those previously obtained for ^{64}Cu-Tz-NOTA: 77 ± 3% intact after 1 h, 47 ± 2% intact after 2 h, and 22 ± 3% intact after 6 h. In all cases, the decomposition of the radioligands resulted in the creation of a poorly resolved array of more hydrophilic catabolites that elute at lower R_f values. The release of $^{64}Cu^{2+}$ from the chelator was not observed in any of the trials.

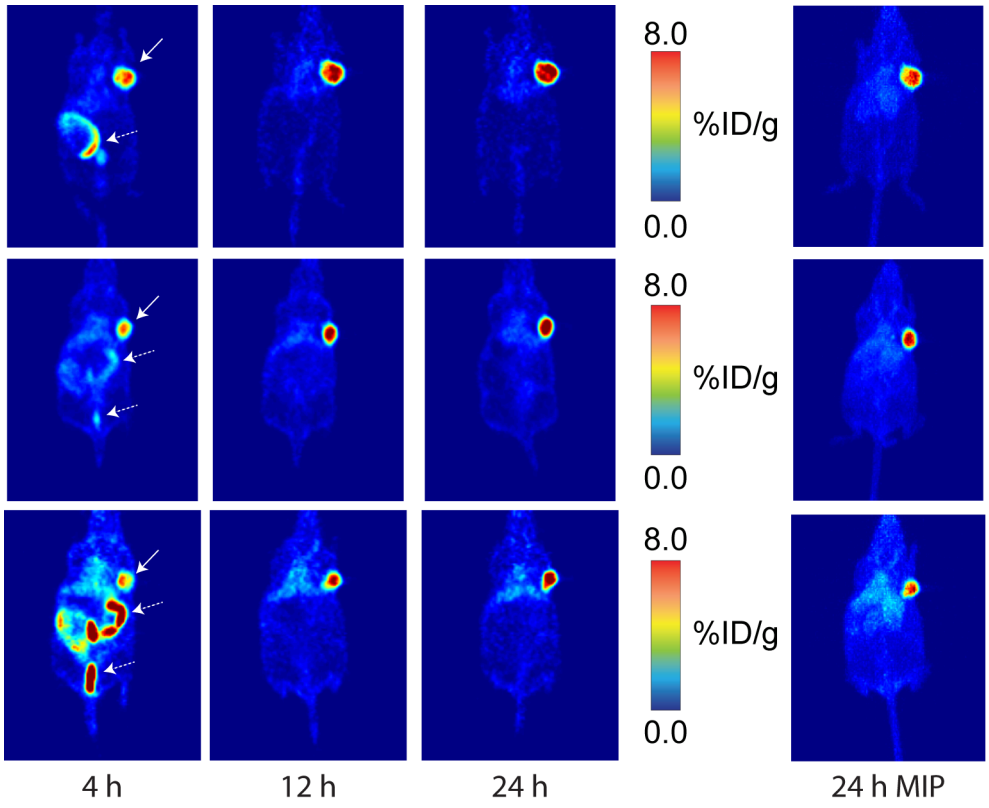

Figure S12. Pretargeted PET imaging using ^{64}Cu-Tz-PEG$_7$-NOTA and a 24 h accumulation interval. Female athymic nude mice (n = 5) bearing subcutaneous SW1222 (right shoulder) xenografts (100-150 mm^3, 18-21 days post-inoculation) were administered 100 μg (0.66 nmol) huA33-TCO (in 200 μL 0.9% sterile saline) via intravenous tail vein injection. After an accumulation interval of 24 h, the same mice were then administered ^{64}Cu-Tz-PEG$_7$-NOTA (400-450 μCi in 200 μL 0.9% sterile saline), also via intravenous tail vein injection (t = 0). The specific activity of ^{64}Cu-Tz-PEG$_7$-NOTA was adjusted using cold ^{nat}Cu-Tz-PEG$_7$-NOTA such that the molar ratio of Tz$_{injected}$:huA33$_{injected}$ = 1:1. Static scans were recorded at various time points after injection with a minimum of 30 million coincident events (10-30 min total scan time). Activity concentrations (percentage of dose per gram of tissue [%ID/g]) and maximum intensity projections were determined by conversion of the counting rates from the reconstructed images. All of the resulting PET images were analyzed using ASIPro VM™ software. The coronal slices intersect the center of the tumor (solid white arrow), and the maximum intensity projection (MIP) displayed was collected at 24 h post-injection. Note the activity not only in the SW1222 xenograft but also in the gut of the mouse (dashed white arrow) at 4 h post-injection.

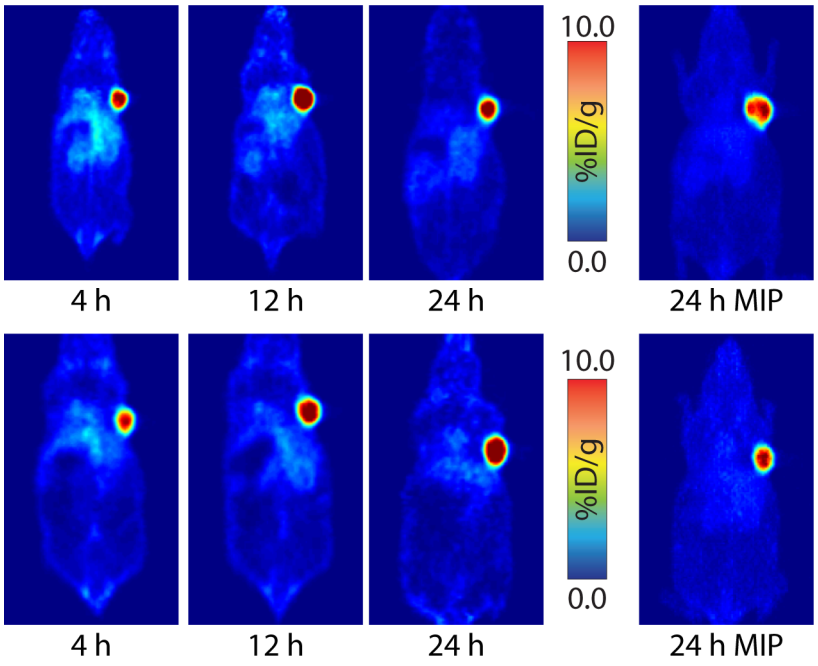

Figure S13. Pretargeted PET imaging using ^{64}Cu-Tz-SarAr and a 24 h accumulation interval. Female athymic nude mice (n = 5) bearing subcutaneous SW1222 (right shoulder) xenografts (100-150 mm^3, 18-21 days post-inoculation) were administered 100 μg (0.66 nmol) huA33-TCO (in 200 μL 0.9% sterile saline) via intravenous tail vein injection. After an accumulation interval of 24 h, the same mice were then administered ^{64}Cu-Tz-SarAr (400-450 μCi in 200 μL 0.9% sterile saline), also via intravenous tail vein injection (t = 0). The specific activity of ^{64}Cu-Tz-SarAr was adjusted using cold ^{nat}Cu-Tz-SarAr such that the molar ratio of $Tz_{injected}$:$huA33_{injected}$ = 1:1. Static scans were recorded at various time points after injection with a minimum of 30 million coincident events (10-30 min total scan time). Activity concentrations (percentage of dose per gram of tissue [%ID/g]) and maximum intensity projections were determined by conversion of the counting rates from the reconstructed images. All of the resulting PET images were analyzed using ASIPro VM™ software. The coronal slices intersect the center of the tumor, and the maximum intensity projection (MIP) displayed was collected at 24 h post-injection.

	1 h	4 h	12 h	24 h
Blood	4.20 ± 0.80	4.00 ± 0.37	2.19 ± 0.39	2.61 ± 0.20
Tumor	5.63 ± 0.67	5.56 ± 0.91	6.74 ± 1.26	7.38 ± 2.02
Heart	1.81 ± 0.46	1.45 ± 0.03	0.84 ± 0.1	0.81 ± 0.04
Lung	1.65 ± 0.51	1.55 ± 0.45	1.24 ± 0.22	0.99 ± 0.24
Liver	1.60 ± 0.12	1.45 ± 0.21	1.33 ± 0.53	1.51 ± 0.2
Spleen	0.98 ± 0.25	0.81 ± 0.20	0.65 ± 0.17	0.64 ± 0.04
Stomach	0.73 ± 0.19	0.56 ± 0.20	0.21 ± 0.1	0.28 ± 0.07
Large Intestine	0.21 ± 0.09	0.48 ± 0.09	0.20 ± 0.04	0.26 ± 0.06
Small Intestine	0.88 ± 0.09	0.62 ± 0.06	0.35 ± 0.08	0.45 ± 0.07
Kidney	3.08 ± 0.28	2.77 ± 0.57	1.87 ± 0.42	2.00 ± 0.24
Muscle	0.38 ± 0.06	0.37 ± 0.07	0.15 ± 0.01	0.20 ± 0.07
Bone	0.67 ± 0.14	0.34 ± 0.18	0.23 ± 0.05	0.29 ± 0.05

Table S10. Biodistribution of ^{64}Cu-Tz-SarAr pretargeting experiment with a 24 h accumulation interval. Female athymic nude mice bearing subcutaneous SW1222 (right shoulder) xenografts (100-150 mm^3, 18-21 days post-inoculation) were administered 100 μg (0.66 nmol) huA33-TCO (in 200 μL 0.9% sterile saline) via intravenous tail vein injection. After an accumulation interval of 24 h, the same mice were then administered ^{64}Cu-Tz-SarAr (300-350 μCi in 200 μL 0.9% sterile saline), also via intravenous tail vein injection (t = 0). The specific activity of the radiotracer was adjusted using cold ^{nat}Cu-Tz-SarAr such that the molar ratio of $Tz_{injected}$:$huA33_{injected}$ = 1:1. Animals (n = 4 per group) were euthanized by CO_2(g) asphyxiation at 1, 4, 12, and 24 h after injection. After asphyxiation, 13 tissues were removed, rinsed in water, dried in air for 5 min, weighed, and counted in a gamma counter calibrated for ^{64}Cu. Counts were converted into activity using a calibration curve generated from known standards. Count data were background- and decay-corrected to the time of injection, and the percent injected dose per gram (%ID/g) for each tissue sample was calculated by normalization to the total activity injected. Stomach, small intestine, and large intestine measurements include contents.

	1 h	4 h	12 h	24 h
Tumor/Blood	1.34 ± 0.30	1.39 ± 0.26	3.07 ± 0.79	2.83 ± 0.81
Tumor/Heart	3.11 ± 0.87	3.84 ± 0.63	8.01 ± 1.77	9.10 ± 2.54
Tumor/Lung	3.40 ± 1.12	3.59 ± 1.20	5.43 ± 1.41	7.44 ± 2.74
Tumor/Liver	3.52 ± 0.49	3.83 ± 0.83	5.06 ± 2.23	4.87 ± 1.48
Tumor/Spleen	5.75 ± 1.61	6.88 ± 2.01	10.34 ± 3.27	11.45 ± 3.20
Tumor/Stomach	7.75 ± 2.24	9.91 ± 3.85	31.76 ± 16.62	26.44 ± 9.89
Tumor/Large Intestine	26.88 ± 12.11	11.65 ± 2.99	33.67 ± 8.82	28.86 ± 10.28
Tumor/Small Intestine	6.42 ± 1.01	8.96 ± 1.71	19.37 ± 5.95	16.33 ± 5.12
Tumor/Kidney	1.83 ± 0.27	2.00 ± 0.53	3.61 ± 1.05	3.68 ± 1.10
Tumor/Muscle	14.92 ± 2.85	14.84 ± 3.69	45.12 ± 8.55	37.37 ± 16.06
Tumor/Bone	8.43 ± 2.07	16.15 ± 8.89	29.8 ± 8.38	25.46 ± 8.22

Table S11. Tumor-to-tissue activity concentration ratios derived from the ^{64}Cu-Tz-SarAr pretargeting biodistribution experiment with a 24 h accumulation interval (*see Table S10*).

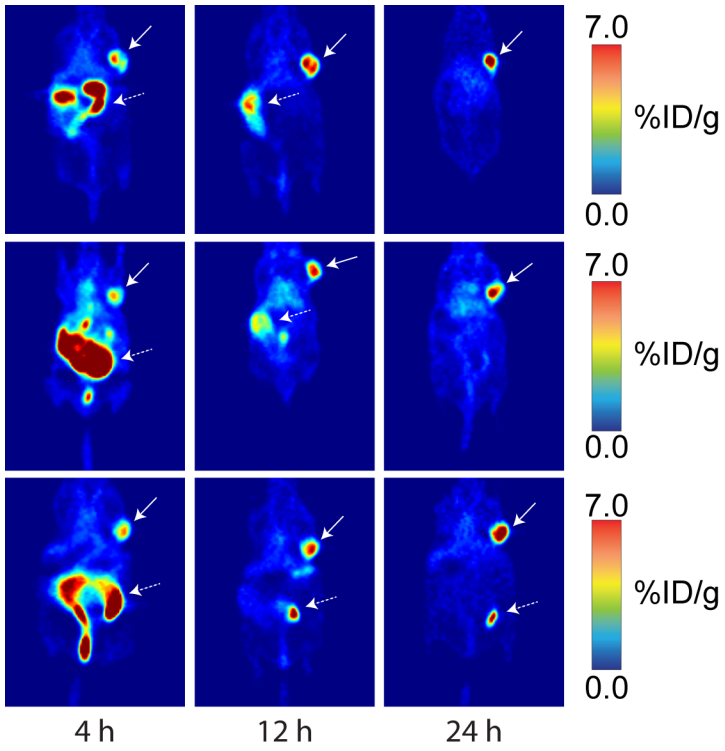

Figure S13. Pretargeted PET imaging using ^{64}Cu-Tz-NOTA. Female athymic nude mice (n = 5) bearing subcutaneous SW1222 (right shoulder) xenografts (100-150 mm^3, 18-21 days post-inoculation) were administered 100 μg (0.66 nmol) huA33-TCO (in 200 μL 0.9% sterile saline) via intravenous tail vein injection. After an accumulation interval of 24 h, the same mice were then administered ^{64}Cu-Tz-NOTA (400-450 μCi in 200 μL 0.9% sterile saline), also via intravenous tail vein injection (t = 0). The specific activity of ^{64}Cu-Tz-NOTA was adjusted using cold ^{nat}Cu-Tz-NOTA such that the molar ratio of $Tz_{injected}$:$huA33_{injected}$ = 1:1. Static scans were recorded at various time points after injection with a minimum of 30 million coincident events (10-30 min total scan time). Activity concentrations (percentage of dose per gram of tissue [%ID/g]) and maximum intensity projections were determined by conversion of the counting rates from the reconstructed images. All of the resulting PET images were analyzed using ASIPro VM™ software. The coronal slices intersect the center of the tumor (solid white arrow), and the maximum intensity projection (MIP) displayed was collected at 24 h post-injection. Note the activity not only in the SW1222 xenograft but also in the gut of the mouse (dashed white arrow) at 4 h post-injection.

	1 h	4 h	12 h	24 h
Blood	3.47 ± 0.63	2.61 ± 0.83	2.31 ± 0.4	2.07 ± 0.49
Tumor	4.07 ± 0.25	4.09 ± 0.61	4.20 ± 0.84	3.94 ± 0.92
Heart	1.09 ± 0.18	0.91 ± 0.27	0.92 ± 0.14	0.82 ± 0.21
Lung	1.58 ± 0.46	1.6 ± 0.39	1.09 ± 0.38	1.03 ± 0.31
Liver	2.19 ± 0.25	1.26 ± 0.3	0.93 ± 0.23	1.07 ± 0.15
Spleen	0.63 ± 0.07	0.51 ± 0.22	0.59 ± 0.25	0.45 ± 0.11
Stomach	0.45 ± 0.08	0.25 ± 0.12	0.52 ± 0.64	0.16 ± 0.03
Large Intestine	13.29 ± 3.15	9.43 ± 4.22	2.92 ± 1.34	1.67 ± 0.88
Small Intestine	0.03 ± 0.04	0.38 ± 0.08	0.77 ± 0.51	0.35 ± 0.04
Kidney	1.3 ± 0.15	0.95 ± 0.31	0.91 ± 0.29	0.7 ± 0.19
Muscle	0.22 ± 0.04	0.14 ± 0.03	0.16 ± 0.02	0.15 ± 0.02
Bone	0.3 ± 0.16	0.27 ± 0.24	0.35 ± 0.11	0.29 ± 0.07

Table S12. Biodistribution of ^{64}Cu-Tz-NOTA pretargeting experiment with a 24 h accumulation interval. Stomach, small intestine, and large intestine measurements include contents. This data was originally published in *JNM*. Zeglis, B. M. *et al.* "A pretargeted PET imaging strategy based on bioorthogonal Diels-Alder click chemistry." *Journal of Nuclear Medicine.* **54**, 1389-1396 (2013). ©2013 by the Society of Nuclear Medicine and Molecular Imaging, Inc.

	1 h	4 h	12 h	24 h
Tumor/Blood	1.17 ± 0.22	1.57 ± 0.55	1.82 ± 0.48	1.9 ± 0.63
Tumor/Heart	3.75 ± 0.65	4.51 ± 1.49	4.58 ± 1.16	4.82 ± 1.69
Tumor/Lung	2.57 ± 0.76	2.55 ± 0.73	3.87 ± 1.55	3.83 ± 1.45
Tumor/Liver	1.86 ± 0.24	3.23 ± 0.9	4.53 ± 1.45	3.69 ± 1.01
Tumor/Spleen	6.46 ± 0.81	7.97 ± 3.57	7.1 ± 3.34	8.79 ± 2.98
Tumor/Stomach	8.96 ± 1.7	16.17 ± 8.21	8.12 ± 10.12	24.29 ± 6.89
Tumor/Large Intestine	0.31 ± 0.08	0.43 ± 0.2	1.44 ± 0.72	2.36 ± 1.37
Tumor/Small Intestine	119.52 ± 148.82	10.83 ± 2.8	5.46 ± 3.81	11.4 ± 2.91
Tumor/Kidney	3.14 ± 0.41	4.32 ± 1.56	4.6 ± 1.71	5.61 ± 1.98
Tumor/Muscle	18.42 ± 3.71	29.38 ± 8.5	26.63 ± 6.59	26.98 ± 7.41
Tumor/Bone	13.72 ± 7.63	14.95 ± 13.2	11.98 ± 4.51	13.43 ± 4.5

Table S13. Tumor-to-tissue activity concentration ratios of ^{64}Cu-Tz-NOTA pretargeting experiment with a 24 h accumulation interval. This data was originally published in *JNM*. Zeglis, B. M. *et al.* "A pretargeted PET imaging strategy based on bioorthogonal Diels-Alder click chemistry." *Journal of Nuclear Medicine.* **54**, 1389-1396 (2013). ©2013 by the Society of Nuclear Medicine and Molecular Imaging, Inc.

Calculation S1. Calculation of the fraction of *in vivo* ligation occurring at the tumor. In order to make an admittedly rough calculation of this value with the available data, two assumptions must be made: (1) that the activity concentration in the tumor at 1 h post-injection is solely the result of *in vivo* click reactions at the tumor and (2) that the activity concentration in the tumor at 24 h post-injection is the maximum total tumor uptake. If we make these two reasonable but likely flawed assumptions, then we can calculate that with a 24 h accumulation interval, 76 ± 23% of the *in vivo* ligations are occurring at the tumor itself. Of course, when the huA33-TCO is given longer amounts of time to accumulate, that fraction goes up: with a 48 h accumulation interval, 93 ± 16% of the *in vivo* ligations are occurring at the tumor, and with a 120 h accumulation interval, 83 ± 22% of the *in vivo* ligations are occurring at the tumor.

Calculation S2. Calculation of the ^{64}Cu-Tz-SarAr/huA33-TCO pretargeting reaction yield. In order to make a rough calculation of this value with the available data, two key assumptions must be made:

(1) That the amount of huA33-TCO present at the tumor 49 hours (48 h accumulation interval + 1 h radiotracer accumulation) after its injection in the pretargeting experiment is approximately equal to the amount of ^{64}Cu-NOTA-huA33 present at the tumor 48 hours after its injection as we determined in our original report.[7]

(2) That the activity concentration in the tumor at 1 h post-injection is solely the result of *in vivo* click reactions at the tumor

With these assumptions in hand, it is possible to make a simple calculation of the yield of the Tz/huA33-TCO reaction at the tumor site. First, if we look back at the biodistribution data for the injection of 100 μg of ^{64}Cu-NOTA-huA33, we can see that the activity concentration at the tumor after 48 h is 4.76 ± 0.83 $\mu Ci/g_{tumor}$. Given that the specific activity of the ^{64}Cu-NOTA-huA33 injected in this experiment was 0.20 $\mu Ci/\mu g_{huA33}$, we can calculate that a total of 23.8 ± 4.1 $\mu g_{huA33}/g_{tumor}$ was present at the tumor at 48 h post-injection, a value equivalent to 0.16 ± 0.03 $nmol_{huA33}/g_{tumor}$ (MW_{huA33} = 150,000).

Now, considering a 48 h pretargeting interval, we can assume that at the time of injection of ^{64}Cu-Tz-SarAr, there is 0.16 ± 0.03 $nmol_{huA33}/g_{tumor}$ of huA33-TCO at the tumor. As we can see from the biodistribution experiment with a 48 h accumulation interval, 1 h after the injection of ^{64}Cu-Tz-SarAr, the activity concentration in the tumor is 12.65 ± 0.91 $\mu Ci/g_{tumor}$. Given that the specific activity of the ^{64}Cu-Tz-SarAr injected in this experiment was 378 $\mu Ci/\mu g_{CuTzSarAr}$, we can calculate that a total of 0.033 ± 0.002 $\mu g_{CuTzSarAr}/g_{tumor}$ was present at the tumor at 1 h post-injection, a value equivalent to 0.043 ± 0.003 $nmol_{TzSarAr}/g_{tumor}$ ($MW_{CuTzSarAr}$ = 780).

Now, we have the concentration of both the huA33-TCO (0.16 ± 0.03 $nmol_{huA33}/g_{tumor}$) and the ^{64}Cu-Tz-SarAr (0.043 ± 0.003 $nmol_{TzSarAr}/g_{tumor}$) at the tumor. The simple ratio of these values will give us the fractional yield of the reaction at the tumor site: 0.27 ± 0.05. Therefore, the yield of the click reaction at the tumor site 27 ± 5% on a per antibody basis. This is generally consistent with the values obtained by other researchers.[8]

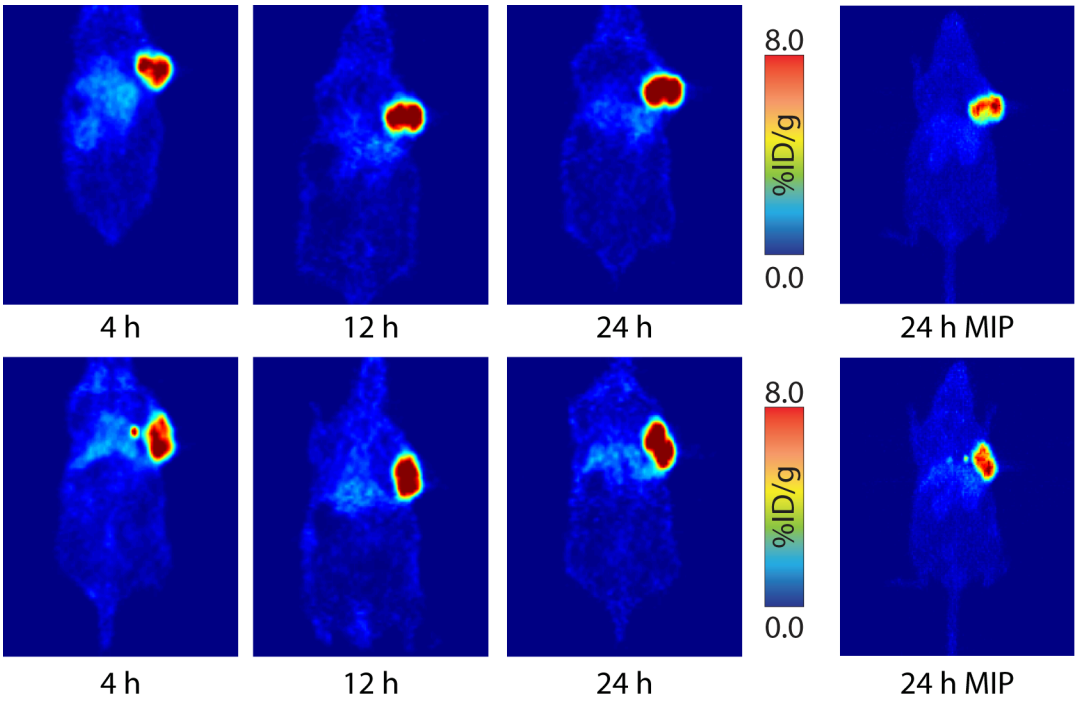

Figure S15. Pretargeted PET imaging using ^{64}Cu-Tz-SarAr and a 48 h accumulation interval. Female athymic nude mice (n = 5 per radioligand) bearing subcutaneous SW1222 (right shoulder) xenografts (100-150 mm^3, 18-21 days post-inoculation) were administered 100 μg (0.66 nmol) huA33-TCO (in 200 μL 0.9% sterile saline) via intravenous tail vein injection. After an accumulation interval of 48 h, the same mice were then administered ^{64}Cu-Tz-SarAr (400-450 μCi in 200 μL 0.9% sterile saline), also via intravenous tail vein injection (t = 0). The specific activity of ^{64}Cu-Tz-SarAr was adjusted using cold ^{nat}Cu-Tz-SarAr such that the molar ratio of $Tz_{injected}$:$huA33_{injected}$ = 1:1. Static scans were recorded at various time points after injection with a minimum of 30 million coincident events (10-30 min total scan time). Activity concentrations (percentage of dose per gram of tissue [%ID/g]) and maximum intensity projections were determined by conversion of the counting rates from the reconstructed images. All of the resulting PET images were analyzed using ASIPro VM™ software. The coronal slices intersect the center of the tumor, and the maximum intensity projection (MIP) displayed was collected at 24 h post-injection.

	1 h	4 h	12 h	24 h
Blood	2.15 ± 0.5	1.78 ± 0.28	1.81 ± 0.54	0.92 ± 0.31
Tumor	4.49 ± 0.44	5.15 ± 1.42	4.94 ± 1.12	4.85 ± 0.67
Heart	1.05 ± 0.24	1.08 ± 0.32	0.88 ± 0.33	0.45 ± 0.08
Lung	1.68 ± 0.09	1.53 ± 0.28	1.00 ± 0.18	1.05 ± 0.51
Liver	1.79 ± 0.09	1.27 ± 0.19	1.08 ± 0.32	1.28 ± 0.33
Spleen	0.84 ± 0.27	0.6 ± 0.09	0.56 ± 0.11	0.5 ± 0.1
Stomach	0.39 ± 0.17	0.27 ± 0.18	0.12 ± 0.04	0.15 ± 0.03
Large Intestine	0.29 ± 0.09	0.41 ± 0.11	0.22 ± 0.08	0.16 ± 0.03
Small Intestine	0.54 ± 0.15	0.33 ± 0.1	0.3 ± 0.08	0.22 ± 0.07
Kidney	1.98 ± 0.26	1.83 ± 0.57	2.04 ± 0.36	1.47 ± 0.43
Muscle	0.22 ± 0.11	0.24 ± 0.08	0.15 ± 0.02	0.11 ± 0.04
Bone	0.23 ± 0.05	0.32 ± 0.12	0.3 ± 0.07	0.18 ± 0.05

Table S14. Biodistribution of ^{64}Cu-Tz-SarAr pretargeting experiment with a 48 h accumulation interval. Female athymic nude mice bearing subcutaneous SW1222 (right shoulder) xenografts (100-150 mm^3, 18-21 days post-inoculation) were administered 100 μg (0.66 nmol) huA33-TCO (in 200 μL 0.9% sterile saline) via intravenous tail vein injection. After an accumulation interval of 48 h, the same mice were then administered ^{64}Cu-Tz-SarAr (300-350 μCi in 200 μL 0.9% sterile saline), also via intravenous tail vein injection (t = 0). The specific activity of the radiotracer was adjusted using cold ^{nat}Cu-Tz-SarAr such that the molar ratio of $Tz_{injected}$:$huA33_{injected}$ = 1:1. Animals (n = 4 per group) were euthanized by CO_2(g) asphyxiation at 1, 4, 12, and 24 h after injection. After asphyxiation, tissues were removed, rinsed in water, dried in air for 5 min, weighed, and counted in a gamma counter calibrated for ^{64}Cu. Counts were converted into activity using a calibration curve generated from known standards. Count data were background- and decay-corrected to the time of injection, and the percent injected dose per gram (%ID/g) for each tissue sample was calculated by normalization to the total activity injected. Stomach, small intestine, and large intestine measurements include contents.

	1 h	4 h	12 h	24 h
Tumor/Blood	2.09 ± 0.52	2.9 ± 0.92	2.72 ± 1.03	5.27 ± 1.92
Tumor/Heart	4.27 ± 1.05	4.75 ± 1.92	5.62 ± 2.47	10.9 ± 2.55
Tumor/Lung	2.67 ± 0.3	3.37 ± 1.11	4.94 ± 1.45	4.61 ± 2.32
Tumor/Liver	2.51 ± 0.27	4.06 ± 1.27	4.58 ± 1.69	3.8 ± 1.11
Tumor/Spleen	5.34 ± 1.79	8.55 ± 2.69	8.75 ± 2.61	9.8 ± 2.47
Tumor/Stomach	11.57 ± 5.25	18.92 ± 13.29	41.88 ± 18.35	32.81 ± 8.37
Tumor/Large Intestine	15.48 ± 5.25	12.68 ± 4.87	22.66 ± 10.19	29.58 ± 6.11
Tumor/Small Intestine	8.35 ± 2.48	15.71 ± 6.48	16.47 ± 5.62	21.72 ± 7.59
Tumor/Kidney	2.27 ± 0.37	2.81 ± 1.16	2.42 ± 0.7	3.31 ± 1.07
Tumor/Muscle	20.34 ± 10.25	21.84 ± 9.2	33.88 ± 9.31	44.18 ± 17.61
Tumor/Bone	19.48 ± 4.94	15.86 ± 7.12	16.24 ± 5.16	26.55 ± 7.58

Table S15. Tumor-to-tissue activity concentration ratios derived from the ^{64}Cu-Tz-SarAr pretargeting biodistribution experiment with a 48 h accumulation interval (*see Table S14*)

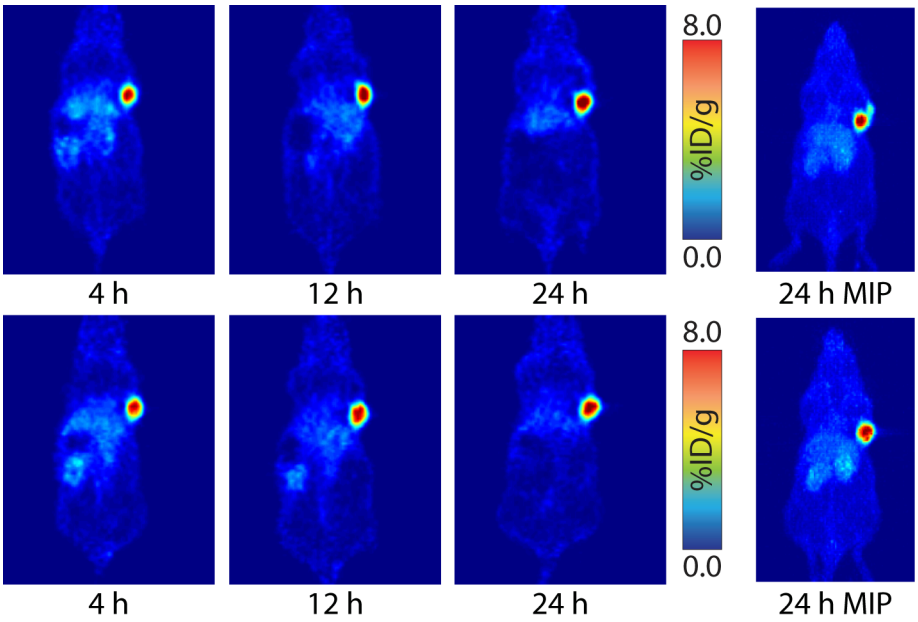

Figure S16. Pretargeted PET imaging using ^{64}Cu-Tz-SarAr and a 120 h accumulation interval. Female athymic nude mice (n = 5) bearing subcutaneous SW1222 (right shoulder) xenografts (100-150 mm^3, 18-21 days post-inoculation) were administered 100 μg (0.66 nmol) huA33-TCO (in 200 μL 0.9% sterile saline) via intravenous tail vein injection. After an accumulation interval of 120 h, the same mice were then administered ^{64}Cu-Tz-SarAr (400-450 μCi in 200 μL 0.9% sterile saline), also via intravenous tail vein injection (t = 0). The specific activity of ^{64}Cu-Tz-SarAr was adjusted using cold ^{nat}Cu-Tz-SarAr such that the molar ratio of $Tz_{injected}$:$huA33_{injected}$ = 1:1. Static scans were recorded at various time points after injection with a minimum of 30 million coincident events (10-30 min total scan time). Activity concentrations (percentage of dose per gram of tissue [%ID/g]) and maximum intensity projections were determined by conversion of the counting rates from the reconstructed images. All of the resulting PET images were analyzed using ASIPro VM™ software. The coronal slices intersect the center of the tumor, and the maximum intensity projection (MIP) displayed was collected at 24 h post-injection.

	1 h	4 h	12 h	24 h
Blood	1.39 ± 0.19	1.05 ± 0.29	0.44 ± 0.14	0.75 ± 0.23
Tumor	3.61 ± 0.45	3.55 ± 0.74	3.29 ± 0.40	4.34 ± 0.98
Heart	0.52 ± 0.06	0.43 ± 0.11	0.34 ± 0.20	0.40 ± 0.16
Lung	1.41 ± 0.21	0.91 ± 0.22	0.59 ± 0.27	0.85 ± 0.29
Liver	1.65 ± 0.07	1.16 ± 0.39	0.96 ± 0.09	1.06 ± 0.16
Spleen	0.60 ± 0.13	0.50 ± 0.05	0.34 ± 0.14	0.69 ± 0.17
Stomach	0.32 ± 0.13	0.25 ± 0.12	0.09 ± 0.03	0.15 ± 0.08
Large Intestine	0.29 ± 0.16	0.20 ± 0.13	0.09 ± 0.03	0.16 ± 0.04
Small Intestine	0.34 ± 0.03	0.22 ± 0.03	0.15 ± 0.07	0.17 ± 0.06
Kidney	1.80 ± 0.12	2.10 ± 0.20	2.11 ± 0.13	1.90 ± 0.17
Muscle	0.20 ± 0.03	0.11 ± 0.05	0.08 ± 0.04	0.14 ± 0.05
Bone	0.21 ± 0.03	0.16 ± 0.04	0.11 ± 0.04	0.25 ± 0.08

Table S16. Biodistribution of ^{64}Cu-Tz-SarAr pretargeting experiment with a 120 h accumulation interval. Female athymic nude mice bearing subcutaneous SW1222 (right shoulder) xenografts (100-150 mm^3, 18-21 days post-inoculation) were administered 100 μg (0.66 nmol) huA33-TCO (in 200 μL 0.9% sterile saline) via intravenous tail vein injection. After an accumulation interval of 120 h, the same mice were then administered ^{64}Cu-Tz-SarAr (300-350 μCi in 200 μL 0.9% sterile saline), also via intravenous tail vein injection (t = 0). The specific activity of the radiotracer was adjusted using cold ^{nat}Cu-Tz-SarAr such that the molar ratio of $Tz_{injected}$:$huA33_{injected}$ = 1:1. Animals (n = 4 per group) were euthanized by CO_2(g) asphyxiation at 1, 4, 12, and 24 h after injection. After asphyxiation, tissues were removed, rinsed in water, dried in air for 5 min, weighed, and counted in a gamma counter calibrated for ^{64}Cu. Counts were converted into activity using a calibration curve generated from known standards. Count data were background- and decay-corrected to the time of injection, and the percent injected dose per gram (%ID/g) for each tissue sample was calculated by normalization to the total activity injected. Stomach, small intestine, and large intestine measurements include contents.

	1 h	4 h	12 h	24 h
Tumor/Blood	2.61 ± 0.48	3.37 ± 1.16	7.46 ± 2.54	5.74 ± 2.17
Tumor/Heart	7.00 ± 1.22	8.24 ± 2.71	9.56 ± 5.64	10.76 ± 4.94
Tumor/Lung	2.55 ± 0.49	3.89 ± 1.23	5.55 ± 2.62	5.09 ± 2.06
Tumor/Liver	2.19 ± 0.29	3.06 ± 1.20	3.43 ± 0.52	4.09 ± 1.13
Tumor/Spleen	6.02 ± 1.46	7.03 ± 1.64	9.63 ± 4.03	6.26 ± 2.09
Tumor/Stomach	11.37 ± 4.88	14.04 ± 7.07	38.07 ± 12.42	29.21 ± 17.97
Tumor/Large Intestine	12.39 ± 7.14	17.82 ± 12.22	35.43 ± 12.17	26.48 ± 8.29
Tumor/Small Intestine	10.53 ± 1.58	16.22 ± 3.91	21.47 ± 9.60	25.34 ± 10.4
Tumor/Kidney	2.01 ± 0.29	1.69 ± 0.39	1.56 ± 0.21	2.29 ± 0.56
Tumor/Muscle	18.41 ± 3.47	32.58 ± 16.17	38.74 ± 20.11	30.39 ± 11.94
Tumor/Bone	17.27 ± 3.03	21.53 ± 7.14	29.07 ± 11.14	17.16 ± 6.90

Table S17. Tumor-to-tissue activity concentration ratios derived from the ^{64}Cu-Tz-SarAr pretargeting biodistribution experiment with a 120 h accumulation interval (*see Table S16*)

Radioligand	^{64}Cu-Tz-NOTA	^{64}Cu-Tz-SarAr		
Accumulation Interval	**24 h**	**24 h**	**48 h**	**120 h**
Tumor/Blood	1.17 ± 0.22	1.34 ± 0.3	2.09 ± 0.52	2.61 ± 0.48
Tumor/Liver	1.86 ± 0.24	3.52 ± 0.49	2.51 ± 0.27	2.19 ± 0.29
Tumor/Large Intestine	0.31 ± 0.08	26.88 ± 12.11	15.48 ± 5.25	12.39 ± 7.14
Tumor/Kidney	3.14 ± 0.41	1.83 ± 0.27	2.27 ± 0.37	2.01 ± 0.29
Tumor/Muscle	18.42 ± 3.71	14.92 ± 2.85	20.34 ± 10.25	18.41 ± 3.47

Table S18. Comparison of salient tumor-to-tissue activity concentration ratios at 1 h post-injection created using the different pretargeted PET imaging strategies discussed (*see Tables S11, S13, S15, and S17*)

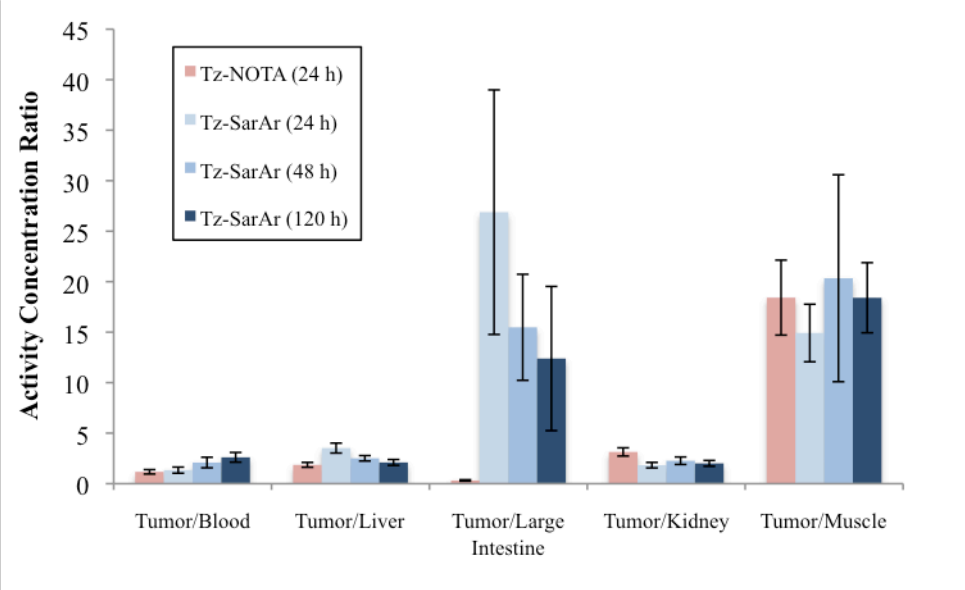

Figure S17. Graphical comparison of salient tumor-to-tissue activity concentration ratios at 1 h post-injection created using the different pretargeted PET imaging strategies discussed (*see Tables S11, S13, S15, S17, and S18*)

Radioligand	^{64}Cu-Tz-NOTA	^{64}Cu-Tz-SarAr		
Accumulation Interval	**24 h**	**24 h**	**48 h**	**120 h**
Tumor/Blood	1.57 ± 0.55	1.39 ± 0.26	2.9 ± 0.92	3.37 ± 1.16
Tumor/Liver	3.23 ± 0.9	3.83 ± 0.83	4.06 ± 1.27	3.06 ± 1.2
Tumor/Large Intestine	0.43 ± 0.2	11.65 ± 2.99	12.68 ± 4.87	17.82 ± 12.22
Tumor/Kidney	4.32 ± 1.56	2.00 ± 0.53	2.81 ± 1.16	1.69 ± 0.39
Tumor/Muscle	29.38 ± 8.5	14.84 ± 3.69	21.84 ± 9.2	32.58 ± 16.17

Table S19. Comparison of salient tumor-to-tissue activity concentration ratios at 4 h post-injection created using the different pretargeted PET imaging strategies discussed (*see Tables S11, S13, S15, and S17*)

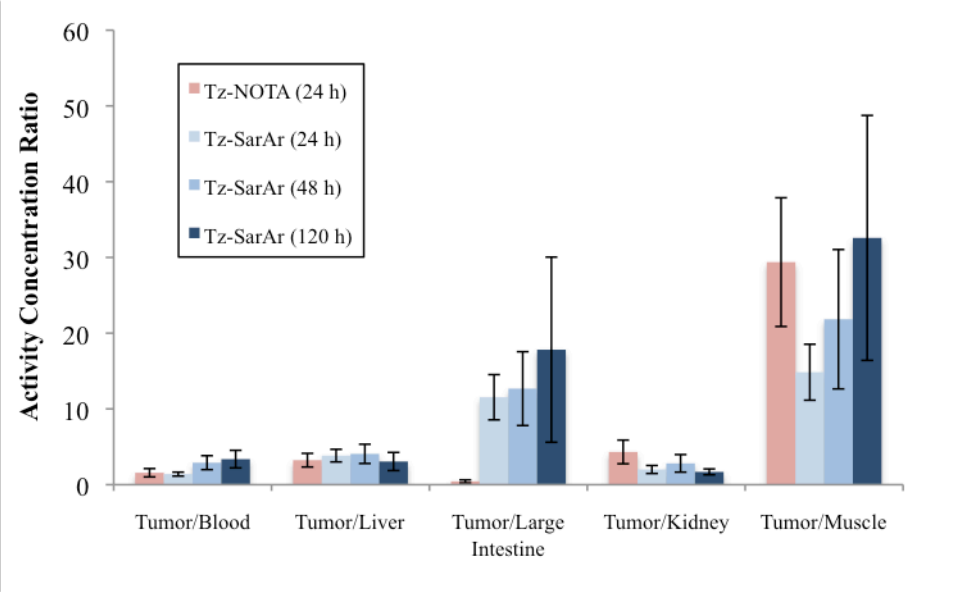

Figure S18. Graphical comparison of salient tumor-to-tissue activity concentration ratios at 4 h post-injection created using the different pretargeted PET imaging strategies discussed (*see Tables S11, S13, S15, S17, and S19*)

Radioligand	^{64}Cu-Tz-NOTA	^{64}Cu-Tz-SarAr		
Accumulation Interval	**24 h**	**24 h**	**48 h**	**120 h**
Tumor/Blood	1.82 ± 0.48	3.07 ± 0.79	2.72 ± 1.03	7.46 ± 2.54
Tumor/Liver	4.53 ± 1.45	5.06 ± 2.23	4.58 ± 1.69	3.43 ± 0.52
Tumor/Large Intestine	1.44 ± 0.72	33.67 ± 8.82	22.66 ± 10.19	35.43 ± 12.17
Tumor/Kidney	4.6 ± 1.71	3.61 ± 1.05	2.42 ± 0.7	1.56 ± 0.21
Tumor/Muscle	26.63 ± 6.59	45.12 ± 8.55	33.88 ± 9.31	38.74 ± 20.11

Table S20. Comparison of salient tumor-to-tissue activity concentration ratios at 12 h post-injection created using the different pretargeted PET imaging strategies discussed (*see Tables S11, S13, S15, and S17*)

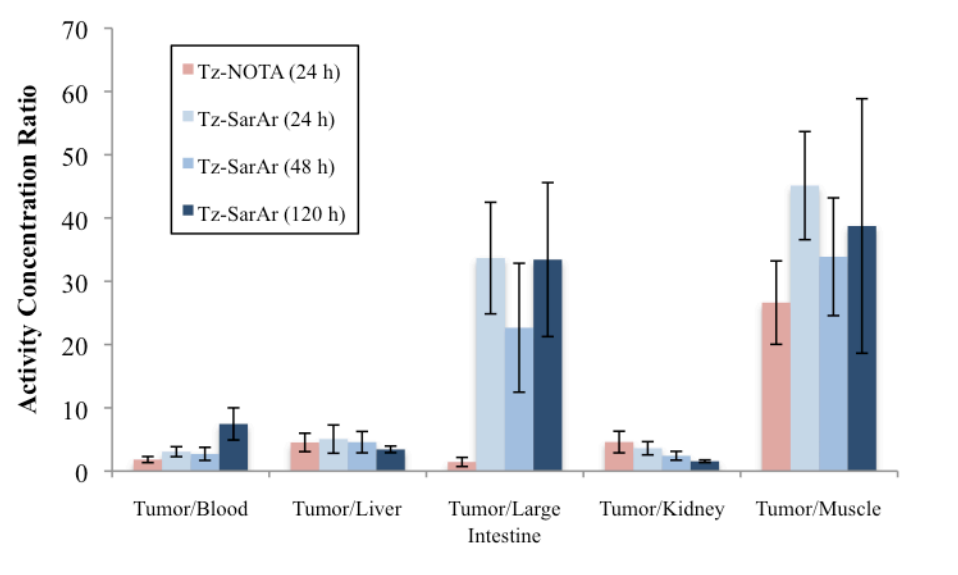

Figure S19. Graphical comparison of salient tumor-to-tissue activity concentration ratios at 12 h post-injection created using the different pretargeted PET imaging strategies discussed (*see Tables S11, S13, S15, S17, and S20*)

Radioligand	^{64}Cu-Tz-NOTA	^{64}Cu-Tz-SarAr		
Accumulation Interval	**24 h**	**24 h**	**48 h**	**120 h**
Tumor/Blood	1.9 ± 0.63	2.83 ± 0.81	5.27 ± 1.92	5.74 ± 2.17
Tumor/Liver	3.69 ± 1.01	4.87 ± 1.48	3.8 ± 1.11	4.09 ± 1.13
Tumor/Large Intestine	2.36 ± 1.37	28.86 ± 10.28	29.58 ± 6.11	26.48 ± 8.29
Tumor/Kidney	5.61 ± 1.98	3.68 ± 1.1	3.31 ± 1.07	2.29 ± 0.56
Tumor/Muscle	26.98 ± 7.41	37.37 ± 16.06	44.18 ± 17.61	30.39 ± 11.94

Table S21. Comparison of salient tumor-to-tissue activity concentration ratios at 24 h post-injection created using the different pretargeted PET imaging strategies discussed (*see Tables S11, S13, S15, and S17*)

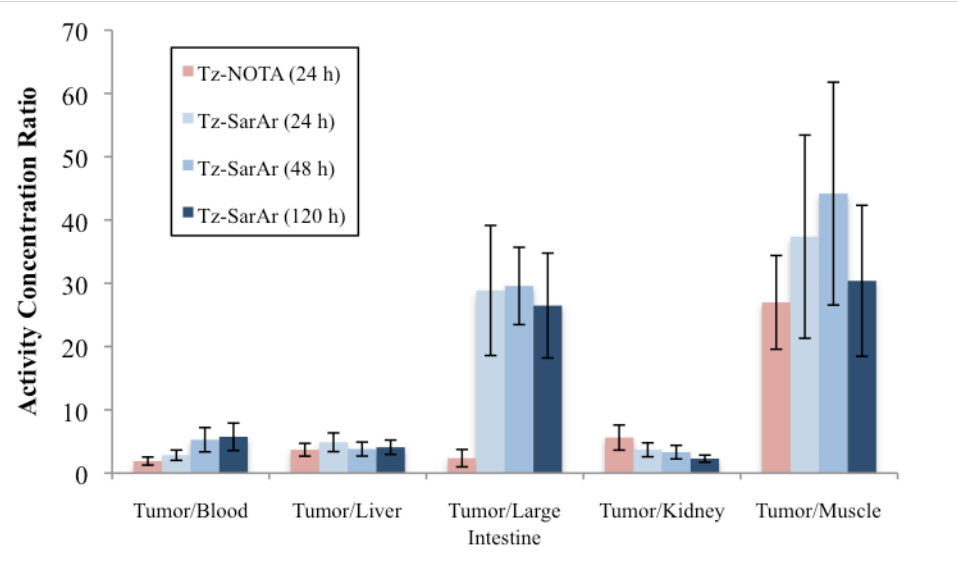

Figure S20. Graphical comparison of salient tumor-to-tissue activity concentration ratios at 24 h post-injection created using the different pretargeted PET imaging strategies discussed (*see Tables S11, S13, S15, S17, and S21*)

Table S22. Dosimetry calculations for various huA33-based PET imaging strategies

Target Organ[†]	^{89}Zr-DFO-huA33[*]	^{64}Cu-NOTA-huA33[*]	Pretargeting			
			^{64}Cu-Tz-NOTA[*]	^{64}Cu-Tz-SarAr		
			24 h interval	*24 h interval*	*48 h interval*	*120 h interval*
Adrenals	0.4432	0.0196	0.0068	0.0101	0.0094	0.0087
Brain	0.2065	0.0150	0.0064	0.0098	0.0092	0.0085
Breasts	0.1678	0.0138	0.0056	0.0088	0.0082	0.0076
Gallbladder Wall	0.3892	0.0200	0.0074	0.0106	0.0099	0.0092
Lower Lg. Int. Wall	0.3622	0.0522	0.0449	0.0131	0.0123	0.0108
Small Intestine	0.3000	0.0225	0.0089	0.0114	0.0105	0.0098
Stomach Wall	0.2565	0.0239	0.0072	0.0127	0.0104	0.0097
Upper Lg. Int. Wall	0.3243	0.0392	0.0308	0.0111	0.0103	0.0096
Heart Wall	0.4189	0.0292	0.0079	0.0116	0.0102	0.0089
Kidneys	0.6838	0.0503	0.0085	0.0178	0.0145	0.0153
Liver	0.7676	0.0524	0.0084	0.0081	0.0090	0.0081
Lungs	0.6108	0.0484	0.0078	0.0088	0.0088	0.0058
Muscle	0.3432	0.0148	0.0037	0.0052	0.0044	0.0038
Ovaries	0.2946	0.0184	0.0081	0.0109	0.0101	0.0094
Pancreas	0.3703	0.0191	0.0070	0.0106	0.0098	0.0091
Red Marrow	0.8432	0.0832	0.0143	0.0082	0.0076	0.0070
Osteogenic Cells	1.6459	0.1186	0.0230	0.0242	0.0218	0.0194
Skin	0.1830	0.0125	0.0052	0.0081	0.0075	0.0069
Spleen	0.6811	0.0324	0.0049	0.0039	0.0032	0.0030
Testes	0.1846	0.0141	0.0061	0.0094	0.0087	0.0081
Thymus	0.2670	0.0158	0.0061	0.0095	0.0088	0.0081
Thyroid	0.2559	0.0152	0.0062	0.0096	0.0089	0.0082
Bladder Wall	0.2232	0.0165	0.0071	0.0106	0.0099	0.0091
Uterus	0.2543	0.0176	0.0075	0.0112	0.0103	0.0096
Total Body	0.3757	0.0231	0.0074	0.0103	0.0094	0.0085
Effective Dose	**0.4162**	**0.0359**	**0.0124**	**0.0112**	**0.0102**	**0.0092**

[†]Mean organ absorbed doses and effective dose are expressed in mGy/MBq and mSv/MBq, respectively.

[*]Data originally reported in Zeglis, B. M. *et al*. *Journal of Nuclear Medicine*. **54**, 1389-1396 (2013).

References

1. Lindmo, T.; Boven, E.; Cuttitta, F.; Fedorko, J.; Bunn, P. A., Jr., Determination of the immunoreactive fraction of radiolabeled monoclonal antibodies by linear extrapolation to binding at infinite antigen excess. *J. Immunol. Methods* **1984,** *72* (1), 77-89.
2. Lindmo, T.; Bunn, P. A., Jr., Determination of the true immunoreactive fraction of monoclonal antibodies after radiolabeling. *Methods Enzymol.* **1986,** *121* (1), 678-91.
3. Oehler, C.; O'Donoghue, J. A.; Russell, J.; Zanzonico, P.; Lorenzen, S.; Ling, C. C.; Carlin, S., 18F-fluromisonidazole PET imaging as a biomarker for the response to 5,6-dimethylxanthenone-4-acetic acid in colorectal xenograft tumors. . *J. Nucl. Med.* **2011,** *52* (3), 437-44.
4. Carlin, S.; Zhang, H.; Reese, M.; Ramos, N. N.; Chen, Q.; Ricketts, S. A., A comparison of the imaging characteristics and microregional distribution of 4 hypoxia PET tracers. *J. Nucl. Med.* **2014,** *55* (3), 515-521.
5. Cristy, M.; Eckerman, K. *Specific absorbed fractions of energy at various ages from internal photon sources (I-VII)*; National technical Information Service, Department of Commerce: Springfield, VA, 1987.
6. Stabin, M. G.; Sarks, R. B.; Crowe, E., OLINDA/EXM: The second-generation personal computer software for internal dose assessment in nuclear medicine. *J. Nucl. Med.* **2005,** *45* (6), 1023-1027.
7. Zeglis, B. M.; Sevak, K. K.; Reiner, T.; Mohindra, P.; Carlin, S.; Zanzonico, P.; Weissleder, R.; Lewis, J. S., A pretargeted PET imaging strategy based on bioorthgonal Diels-Alder click chemistry. *J. Nucl. Med.* **2013,** *54*, 1389-1396.
8. Rossin, R.; Lappchen, R.; van den Bosch, S. M.; LaForest, R.; Robillard, M. S., Diels-Alder reaction for tumor pretargeting: In vivo chemistry can boost tumor radiation dose compared with directly labeled antibody. *J. Nucl. Med.* **2013,** *54*, 1989-1995.